Finite-Temperature Investigation of Ferroelectric Solid Solutions from First-Principles: Application to the Structural Properties of $Pb(Zr_{0.5}Ti_{0.5})O_3$

L. Bellaiche,[1] Alberto García[2] and David Vanderbilt[3]

[1] *Physics Department, University of Arkansas, Fayetteville, Arkansas 72701, USA*
[2] *Departamento de Fisica Aplicada II, Universidad del Pais Vasco, Apartado 644, 48080 Bilbao, Spain*
[3] *Center for Materials Theory, Department of Physics and Astronomy, Rutgers University, Piscataway, New Jersey 08854-8019, USA*

Abstract. The first-principles-derived approach proposed in Ref. [1] is used to study structural properties of $Pb(Zr_{0.5}Ti_{0.5})O_3$ alloys at finite-temperature. Predictions are in excellent agreement with experimental data and direct first-principles results. Other possibilities offered by this approach are also discussed.

INTRODUCTION

Ferroelectric materials are of growing importance for a variety of device applications. Examples include piezoelectric transducers, actuators, and non-volatile ferroelectric memories, as well as dielectrics for microelectronics and wireless communication. The perovskite oxides ABO_3 (e.g., $PbTiO_3$) comprise an important class of ferroelectric materials. At high temperature, these share the paraelectric simple-cubic perovskite structure: metal A atoms at the cube corners, metal B atoms at the cube centers, and O atoms at the cube face centers. As the temperature is reduced, many of the perovskite compounds undergo structural phase transitions and develop a switchable spontaneous electric polarization $\mathbf{P}$, thus becoming ferroelectric.

Most of the perovskite compounds that are of greatest technological interests are not simple systems, but rather $A(B',B'')O_3$ alloys with two different kinds of B atoms. For example, $Pb(Zr,Ti)O_3$ alloys are currently used in piezoelectric transducers and actuators [2]. Similarly, the use of $Ba(Zn,Ta)O_3$ and $Ba(Mg,Ta)O_3$ alloys as dielectric resonators greatly improve the performance of the high-frequency

wireless technologies [3], such as cellular phones and global positioning systems. Last but not least, the compounds $Pb(Mg,Nb)O_3$ and $Pb(Zn,Nb)O_3$ exhibit such extraordinarily high values of the piezoelectric constants when alloyed with $PbTiO_3$ [4] that they could usher in a new generation of piezoelectric devices [5]. Very little is known about the microscopic behavior that is responsible for the fascinating and anomalous properties of these ferroelectric alloys.

Since the early 1990's, first-principles methods have emerged as one of the most powerful tools for the theoretical investigation of the properties of ferroelectric systems (see [6–9] and references therein). However, these methods are essentially restricted to the study of the zero-temperature properties, while technological applications and fundamental features – such as phase transitions – are realized at finite temperature. Moreover, because of computational cost, only structures containing a small number of atoms per unit cell can be investigated directly via first-principles methods, while accurate prediction of alloy properties would require calculations on much larger cells. Ideally, one would like to have a computational scheme with the capability of predicting the properties of "real" perovskite alloy systems at finite-temperature, with the accuracy of the first-principles methods. Such a computational scheme has recently been proposed in Ref. [1].

The aim of this article is to test this scheme by investigating the structural properties of the $Pb(Zr_{0.5}Ti_{0.5})O_3$ (PZT) alloy at finite temperature. We chose this alloy as a test case because experimental data, as well as direct first-principles results, are available for it. A direct comparison with these data and results will thus attest to the accuracy of the proposed computational scheme.

This article is organized as follows. Section II recapitulates our theoretical approach. Results are shown and discussed in Section III. Finally, new possibilities offered by this numerical technique are detailed in Section IV.

CONSTRUCTION OF THE FINITE-TEMPERATURE COMPUTATIONAL SCHEME FROM FIRST-PRINCIPLES

We construct an effective Hamiltonian based on first-principles calculations as follows. For a *ferroelectric* material, the effective Hamiltonian should include structural degrees of freedom corresponding to the ferroelectric local soft mode and the strain variables. These are the most important degrees of freedom because ferroelectric transitions are accompanied by a softening of the phonon soft mode and by the appearance of a strain [10]. Moreover, a realistic *alloy* effective Hamiltonian must also include the compositional degrees of freedom, because the atomic arrangement can strongly affect the ferroelectric properties of an alloy [11]. We propose to incorporate all such degrees of freedom by writing the total energy E as a sum of two energies,

$$E(\{\mathbf{u}_i\},\{\mathbf{v}_i\},\eta_H,\{\sigma_j\}) \;=\; E_{\rm ave}(\{\mathbf{u}_i\},\{\mathbf{v}_i\},\eta_H) \;+\; E_{\rm loc}(\{\mathbf{u}_i\},\{\mathbf{v}_i\},\{\sigma_j\}) \;\;, \quad (1)$$

where $\mathbf{u}_i$ is the local soft mode in unit cell i; $\{\mathbf{v}_i\}$ are the dimensionless local displacements which are related to the inhomogeneous strain variables inside each cell [10]; η_H is the homogeneous strain tensor; and the $\{\sigma_j\}$ characterize the atomic configuration of the alloy. That is, σ_j=+1 or −1 corresponds to the presence of a B′ or B″ atom, respectively, at lattice site j of the $A(B'_{1-x}B''_x)O_3$ alloy. The energy $E_{\rm ave}$ depends only on the soft mode and strain variables. The $\{\sigma_j\}$ parameters are thus incorporated into the second energy term $E_{\rm loc}$.

Analytical expressions for the total energy E have been recently developed [10,12] for *simple* ABO_3 perovskite systems (i.e., in the absence of $\{\sigma_j\}$ variables). These have been very successful both for reproducing phase transition sequences [10,12,13] and for studying ferroelectric domain walls [14], as well as for calculating finite-temperature dielectric and electromechanical properties [15–17]. Here, for $E_{\rm ave}$, we generalize the analytical expression of Ref. [10] to the case of an $A(B'_{1-x},B''_x)O_3$ alloy, by making use of the virtual crystal approximation (VCA) [18–20]. We thus replace $A(B'_{1-x},B''_x)O_3$ by a virtual (uniform) ABO_3 system in which the potential felt by the electrons is a compositional average of the potentials felt by the electrons in the $AB'O_3$ and $AB''O_3$ parent systems. $E_{\rm ave}$ thus consists of five parts: a local-mode self-energy, a long-range dipole-dipole interaction, a short-range interaction between soft modes, an elastic energy, and an interaction between the local modes and local strain [10]. The analytical expression for $E_{\rm ave}$ has 18 free parameters (see Table II of Ref. [10]) that are determined by fitting to the results of almost 40 first-principles calculations on small VCA cells (typically between 5 and 20 atoms/cell) following the procedure of Ref. [10].

While expressions were available for $E_{\rm ave}$, we were not aware of any analytical expression that had previously been proposed and tested for $E_{\rm loc}$. Following the spirit of the "computational alchemy" method developed for calculating the compositional energy of semiconductor alloys [21–23], we derived $E_{\rm loc}$ by treating the alloy configuration $\{\sigma_j\}$ as a perturbation of the VCA system. We adopted an expression that includes: (i) the *on-site* effect of alloying on the self-energy up to the fourth order in the local mode amplitude $\mathbf{u}_i$; and (ii) the *intersite* contributions involving the first-order terms in a perturbation expansion in powers of σ_j (i.e., terms that are linear in $\mathbf{u}_i$ or $\mathbf{v}_i$). That is,

$$
\begin{aligned}
&E_{\rm loc}(\{\mathbf{u}_i\},\{\mathbf{v}_i\},\{\sigma_j\}) = \\
&\quad \sum_i [\Delta\alpha(\sigma_i)\ u_i^4 \ + \ \Delta\gamma(\sigma_i)\ (u_{ix}^2 u_{iy}^2 + u_{iy}^2 u_{iz}^2 + u_{iz}^2 u_{ix}^2)] \\
&\quad + \ \sum_{ij} [Q_{j,i}\ \mathbf{e}_{ji}\cdot\mathbf{u}_i \ + \ R_{j,i}\ \mathbf{f}_{ji}\cdot\mathbf{v}_i)] \ , \qquad (2)
\end{aligned}
$$

where the sum over i runs over all the unit cells, while the sum over j runs over the mixed sublattice sites. $\Delta\alpha(\sigma_i)$ and $\Delta\gamma(\sigma_i)$ characterize the on-site contribution of alloying, while $Q_{j,i}$ and $R_{j,i}$ are related to alloy-induced intersite interactions. u_{ix}, u_{iy} and u_{iz} are the Cartesian coordinates of the local-mode $\mathbf{u}_i$. $\mathbf{e}_{ji}$ is a unit vector joining the site j to the center of the soft mode $\mathbf{u}_i$, and $\mathbf{f}_{ji}$ is a unit vector

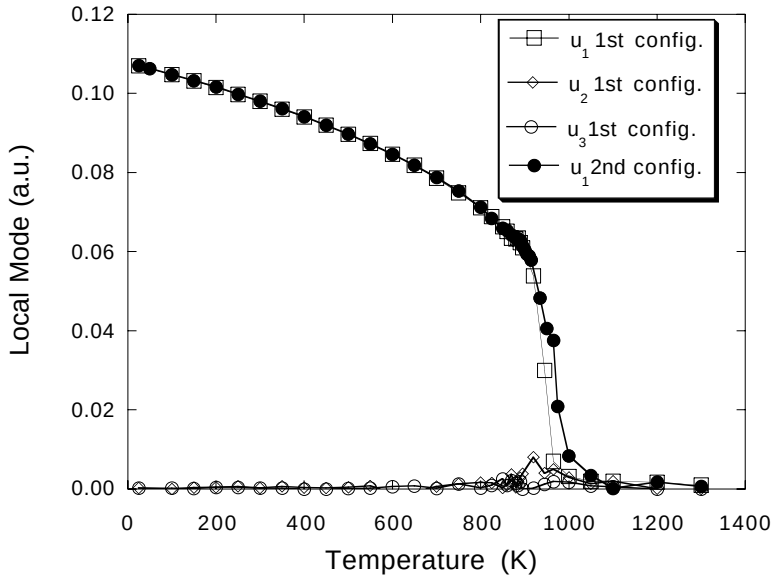

FIGURE 1. The averaged largest, middle and smallest Cartesian coordinates u_1, u_2 and u_3 of the supercell-averaged local mode amplitude as a function of temperature in disordered single crystals of $Pb(Zr_{0.5}Ti_{0.5})O_3$. The open and filled symbols refer to two different random atomic configurations. (For clarity, the u_2 and u_3 of the second configuration are not shown; they are nearly null at all temperatures.) The supercell size is $10\times10\times10$.

joining the site j to the origin of $\mathbf{v}_i$. In principle, terms involving higher powers of $\{\sigma_j\}$, $\mathbf{u}_i$ and $\mathbf{v}_i$ might be included to improve the quality of the expansion, but as we will show below, we find this level of expansion to give a very good account of experimental findings. We also find that $\mathrm{Q}_{j,i}$ and $\mathrm{R}_{j,i}$ rapidly decrease as the distance between i and j increases. As a result, we included the contribution up to the third neighbors for $\mathrm{Q}_{j,i}$, and up to the first neighbor shell for $\mathrm{R}_{i,j}$. Note that for symmetry reasons, the expression for the intersite interactions becomes more complex when going beyond the third neighbor shell.

The quantities $\Delta\alpha(\sigma_i)$, $\Delta\gamma(\sigma_i)$, $\mathrm{Q}_{j,i}$ and $\mathrm{R}_{j,i}$ are derived by performing first-principles calculations in which a true atom [e.g., Ti or Zr in $Pb(Zr,Ti)O_3$] is surrounded by VCA atoms. The *first-principles* method used in the present study here to fully specify the effective Hamiltonian is the plane-wave ultrasoft-pseudopotentials method [24] within the local-density approximation (LDA) [25]. The virtual crystal approximation used is the one proposed in Ref. [19].

Once our effective Hamiltonian is fully specified, the total energy of Eq. (1) is used in Monte-Carlo simulations to compute *finite-temperature* properties of ferroelectric alloys. The $\{\sigma_j\}$ variables are chosen randomly in order to mimic maximal compositional disorder – consistent with the experiment – and are kept fixed during the Monte-Carlo simulations. The outputs of the Monte-Carlo procedure are the

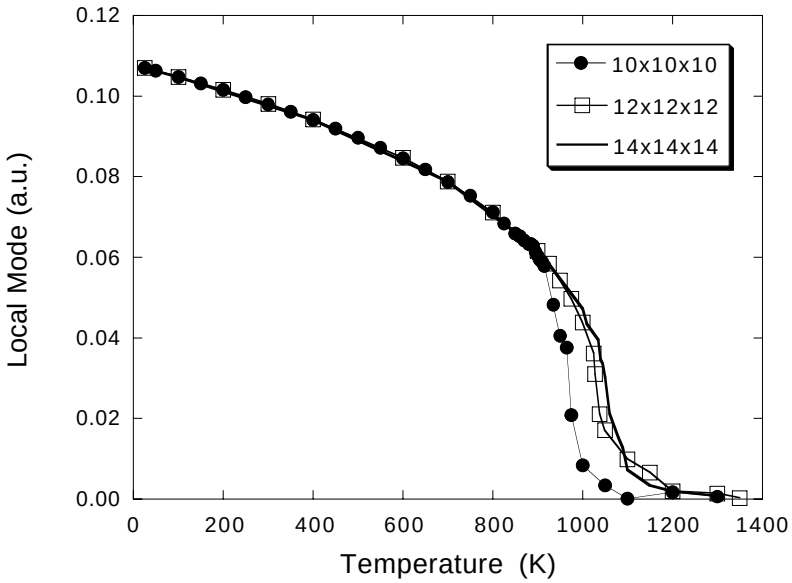

FIGURE 2. The largest Cartesian coordinate u_1 of the average local mode amplitude as a function of temperature. Filled and open symbols refer to 10×10×10 and 12×12×12 supercells respectively, while the solid line indicates the prediction for a 14×14×14 supercell. For each supercell size, only one random configuration is used. The other Cartesian coordinates (u_2 and u_3) are not shown, and are nearly null at all temperatures.

cell-averaged local mode amplitude **u** (which is directly proportional to the electrical polarization) and the homogeneous strain η_H. Up to 10^6 Monte-Carlo sweeps are first performed to equilibrate the system, and then 2×10^4 Monte Carlo sweeps are used to get the various statistical averages. The system is cooled down in small steps.

RESULTS

Figure 1 shows the largest, middle and smallest Cartesian cubic coordinates u_1, u_2 and u_3 of the local mode of $Pb(Zr_{0.5}Ti_{0.5})O_3$ as a function of temperature, as predicted by our approach of Eqs. (1) and (2). Here, we use a 10×10×10 supercell, corresponding to 5000 atoms, to perform the Monte-Carlo simulations. The predictions for two different realizations of the disorder are shown. One can notice that the results are fairly independent of the configuration used to mimic the randomness. In each case, u_1, u_2 and u_3 are close to zero at high temperature, characterizing a paraelectric cubic phase. u_1 then drastically increases at around 950 K, while u_2 and u_3 remain nearly null as the temperature decreases further. The finite-temperature behavior of the phonon local mode amplitude indicates a transition to a ferroelectric tetragonal phase as is experimentally observed [26].

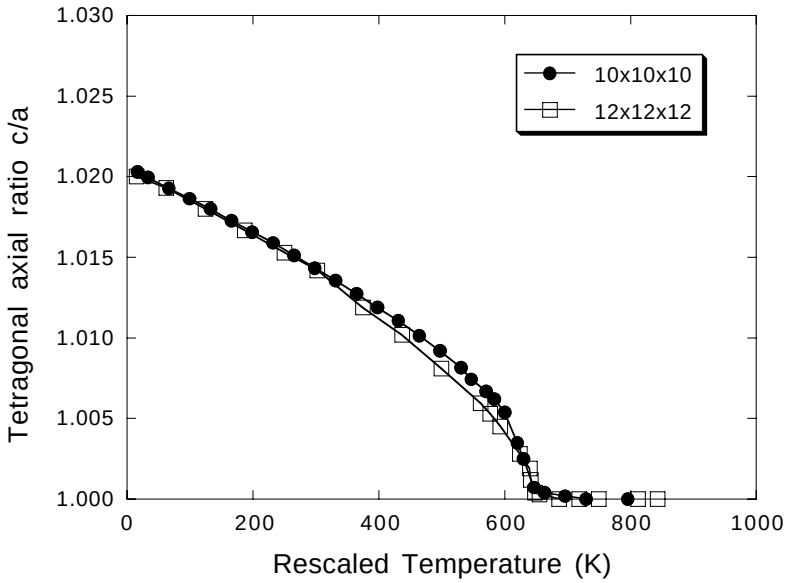

FIGURE 3. The tetragonal axial ratio c/a as a function of temperature in disordered single crystals of $Pb(Zr_{0.5}Ti_{0.5})O_3$. Filled and open symbols refer to $10\times10\times10$ and $12\times12\times12$ supercells, respectively. For each supercell size, only one random configuration is used.

Figure 2 shows the effect of the supercell size on the behavior of the local phonon mode as a function of the temperature. A single realization of the disordered is used for each supercell size. One can clearly see that it is necessary to use a $12\times12\times12$ supercell, corresponding to 8640 atoms, to have convergent results. As a matter of fact, increasing the supercell size from $10\times10\times10$ to $12\times12\times12$ leads to an increase of the Curie temperature T_c by 60 K. On the other hand, increasing even further the size of the supercell to $14\times14\times14$ does not lead to any significant further change of T_c.

All the theoretical Curie temperatures displayed in Figs. 1 and 2 are much higher than the experimental value of 640 K [27]. This difficulty of reproducing T_c seems to be a general feature of the effective-Hamiltonian approach [10,12,13], and may be due to higher perturbative terms not included in the analytical expression for the total energy. This shortcoming can be overcome by multiplying the temperature used in the simulation by a constant factor of $T_{c,exp}/T_{c,theo}$, where $T_{c,exp}$ and $T_{c,theo}$ are the Curie temperatures observed and predicted, respectively [15].

Figure 3 shows that the tetragonal axial ratio c/a looks very similar for the $10\times10\times10$ and $12\times12\times12$ supercells when adopting this temperature rescaling. The c/a ratio is predicted to range from 1 (close to the transition region) to 1.02 (at very low temperature). This is in good agreement both with the experimental value of 1.02-1.025 [26,28] obtained for disordered samples, and with the direct first-principles result of 1.03 obtained for an ordered alloy [8]. Our finite-temperature

TABLE 1. Structural parameters of tetragonal $Pb(Zr_{0.5}Ti_{0.5}O_3)$. 'FTA' denotes the predictions at 50K given by our finite-temperature approach. 'FPO' denotes the direct-first principles calculations for a [100]-ordered supercell (Ref. [8]). 'EXP' denotes the experimental result of Ref. [32]. z are the ferroelectric atomic positions, in c-lattice units. The origin is chosen to be on a Pb atom.

	FTA	FPO	EXP
$z(Pb)$	0.000	0.000	0.000
$z(\langle B\rangle)$	0.442	0.446	0.452
$z(O_1)$	0.376	0.369	0.379
$z(O_3)$	−0.098	−0.104	−0.103

approach is thus able not only to reproduce the correct phase transition sequence but also to predict quite accurately the relevant lattice parameters of PZT. The effective Hamiltonian approach described in Eqs. (1) and (2) is also capable of predicting the internal atomic displacements, since the phonon local-mode u is simply related to them via the eigenvectors of a second derivative matrix [10,29]. Table I demonstrates that these predictions are in excellent agreement both with data measured on disordered samples and with direct first-principles calculations performed on ordered $Pb(Zr_{0.5}Ti_{0.5})O_3$. Note that in Table I, the averaged transition-metal atom interpolating between Zr and Ti is referred to as $\langle B\rangle$, and the oxygen atoms are grouped into two kinds: those denoted O_3, located between two $\langle B\rangle$ atoms along the z direction; and those denoted O_1, located between two $\langle B\rangle$ atoms in the perpendicular directions [7,30].

CONCLUSIONS AND PERSPECTIVES

In summary, the first-principles derived computational approach proposed in Ref. [1] has been tested and used to study structural properties of the $Pb(Zr_{0.5}Ti_{0.5})O_3$ solid solution as a function of temperature. We find that all predicted structural properties – the phase transition sequence, the tetragonal axial ratio, and the internal atomic coordinates – are in very good agreement with measurements and with direct first-principles calculations when available.

Reference [1] demonstrates that this finite-temperature computational scheme also offers other important possibilities. For instance, it confirms the existence of the low-temperature monoclinic phase of PZT experimentally found for Ti compositions ranging between 47% and 50% [28,31,32]. This new scheme also leads to a new explanation for the unusually large value of the piezoelectric coefficient found in tetragonal ceramics of PZT, namely that it arises from a huge value of the d_{15} piezoelectric coefficient that is predicted to occur for a single crystal of PZT [1].

Materials other than PZT, as well as other properties (e.g., the dielectric response), are currently being investigated using this new technique. Once again, preliminary results show a very good agreement with experimental results. In the future, it will be of particular interest to use this approach to investigate the effects

of atomic long-range order, atomic short-range order, and pressure on the structural, piezoelectric and dielectric properties of ferroelectric solid solutions. This scheme may also be used to probe the atomic features responsible for the very intriguing relaxor behavior of some perovskite alloys. Based on its successes and on its broad possibilities, this scheme may help in fulfilling the dream of computational design of new ferroelectric materials.

L.B. thanks the financial assistance provided by the Arkansas Science and Technology Authority (grant N99-B-21), and by the National Science Foundation (grant DMR-9983678). A.G. acknowledges support from the Spanish Ministry of Education (grant PB97-0598). D.V. acknowledges Office of Naval Research grant N00014-97-1-0048. We wish to thank B. Noheda, H. Chen, M. Cohen, E. Cross, T. Egami and Q. Zhang for very useful discussions.

REFERENCES

1. L. Bellaiche, A. García and D. Vanderbilt, submitted to *Phys. Rev. Lett.* (2000).
2. K. Uchino, (Kluwer Academic Publishers, Boston) (1996).
3. M.A. Akbas and P.K. Davies, *J. Am. Ceram. Soc.* **81**, 670 (1998)
4. S.-E. Park and T.E. Shrout, *J. Appl. Phys.*, **82**, 1804 (1997).
5. R.F. Service, *Science*, **275**, 1878 (1997).
6. D. Vanderbilt, *Curr. Opin. Solid State Mater. Sci.*, **2**, 701 (1997).
7. G. Saghi-Szabo, R.E. Cohen and H. Krakauer, *Phys. Rev. B* **59**, 12771 (1999).
8. L. Bellaiche and D. Vanderbilt, *Phys. Rev. Lett.*, **83**, 1347 (1999).
9. L. Bellaiche, J. Padilla and D. Vanderbilt, *Phys. Rev. B.* **59**, 1834 (1999).
10. W. Zhong, D. Vanderbilt and K.M. Rabe, *Phys. Rev. Lett.* **73**, 1861 (19944); *Phys. Rev. B* **52**, 6301 (1995);
11. N. Setter and L.E. Cross, *J. Appl. Phys.* **51**, 4356 (1980).
12. U. Waghmare and K. Rabe, *Phys. Rev. B* **55**, 6161 (1997).
13. H. Krakauer, R. Yu, C.-Z. Wang and C. LaSota, *Ferroelectrics* **206-207**, 133 (1998).
14. J. Padilla, W. Zhong and D. Vanderbilt, *Phys. Rev. B* **53**, R5969 (1996).
15. A. García and D. Vanderbilt, in *First-Principles Calculations for Ferroelectrics: Fifth Williamsburg Workshop*, R.E. Cohen, ed. (AIP, Woodbury, New York, 1998), p. 53.
16. A. García and D. Vanderbilt, *Appl. Phys. Lett.* **72**, 2981 (1998).
17. K.M. Rabe and E. Cockayne, in *First-Principles Calculations for Ferroelectrics: Fifth Williamsburg Workshop*, R.E. Cohen, ed. (AIP, Woodbury, New York, 1998), p. 61.
18. L. Nordheim, *Ann. Phys.* (Leipzig) **9**, 607 (1931).
19. L. Bellaiche and D. Vanderbilt, *Phys. Rev. B*, in press (2000).
20. N. J. Ramer and A. M. Rappe, *J. Phys. Chem. Solids*, **61**, 317 (2000); N. J. Ramer and A. M. Rappe, *Phys. Rev. B*, in preparation (2000).
21. S. de Gironcoli, P. Giannozzi and S. Baroni, *Phys. Rev. Lett.*, **66**, 2116 (1991).
22. N. Marzari, S. de Gironcoli and S. Baroni, *Phys. Rev. Lett.*, **72**, 4001 (1994).
23. A.M. Saitta, S. de Gironcoli, and S. Baroni, *Phys. Rev. Lett.* **80**, 4939 (1998).
24. D. Vanderbilt, *Phys. Rev. B* **41**, 7892 (1990).

25. P. Hohenberg and W. Kohn, *Phys. Rev.* **136**, B864 (1964); W. Kohn and L.J. Sham, *ibid.* **140**, A1133 (1965).
26. M.E. Lines and A.M. Glass, *Principles and Applications of Ferroelectrics and Related Materials* (Clarendon Press, Oxford, 1977).
27. T. Yamamoto, *Jpn. J. Appl. Phys.* **35**, 5104 (1996).
28. B. Noheda, D.E. Cox, G. Shirane, J.A. Gonzalo, L.E. Cross, and S-E. Park, *Appl. Phys. Lett.* **74**, 2059 (1999).
29. R.D. King-Smith and D. Vanderbilt, *Phys. Rev. B* **49**, 5828 (1994).
30. A. García and D. Vanderbilt, *Phys. Rev. B* **54**, 3817 (1996).
31. B. Noheda, J.A. Gonzalo, A. Caballero, C. Moure, D.E. Cox and G. Shirane, unpublished (preprint http://xxx.lanl.gov/abs/cond-mat/9907286).
32. B. Noheda, J.A. Gonzalo, L.E. Cross, R. Guo, S.-E. Park, D.E. Cox and G. Shirane, unpublished (preprint http://xxx.lanl.gov/abs/cond-mat/9910066).